International Journal of Pharmaceutics 414 (2011) 171–178

Contents lists available at ScienceDirect

International Journal of Pharmaceutics

journal homepage: www.elsevier.com/locate/ijpharm

Real-time in-die compaction monitoring of dry-coated tablets

Jingfei Liu, James D. Stephens, Brian R. Kowalczyk, Cetin Cetinkaya*

Department of Mechanical and Aeronautical Engineering, Photo-Acoustics Research Laboratory, Center for Advanced Materials Processing, Wallace H. Coulter School of Engineering, Clarkson University, Potsdam, NY 13699-5725, USA

ARTICLE INFO

Article history:
Received 16 February 2011
Received in revised form 4 May 2011
Accepted 6 May 2011
Available online 14 May 2011

Keywords:
Dry-coated tablets
Real-time quality monitoring systems
In-die online monitoring
Core eccentricity
Process Analytical Technology (PAT)

ABSTRACT

The practicability of a pulse–echo ultrasonic approach developed for the real-time quality monitoring of dry-coated tablets in the tablet press during compaction is evaluated. The punch–tablet interface (i.e., steel–tablet) is the boundary condition that dictates the viability of acoustic in-die compaction monitoring. The current study utilizes compacted tablets with a simulated punch–tablet interface to achieve the required waveform detectability levels needed for in-die compaction monitoring. The geometric and mechanical properties of a dry-coated tablet are crucial to its structural functions and therapeutic effectiveness, therefore they are monitored especially when the control of dissolution rates of their active ingredients are critically important. Acquired pulse–echo ultrasonic waveforms in the tablet could provide the time-of-flight information needed to determine the thickness, elasticity and/or integrity of the relevant layer, and bonding quality between layers depending on the given parameters. Since the amplitudes of the reflected waves are extremely low due to the high acoustic impedance mismatches of tablet materials and die/punch materials, signal processing techniques are required to extract the wave arrival times. In current study, it is demonstrated that the reflection of an ultrasonic pulse generated by a transducer embedded in a die or a punch from the coat–core interface can be acquired by the same transducer.

1. Introduction

The drug tablet and its oral administration remains the most commonly used method of drug delivery in medicine today. In drug delivery devices, such as tablets, maintaining a constant systemic drug concentration within the circulatory system is the key performance metric. The dry-coated tablet dosage form (i.e., the tablet-in-tablet design) is a time- and rate-controlled drug delivery device, which consists of a core tablet and an outer layer that is considerably thicker than typical tablet coats, and which completely surrounds the core (inner) tablet. Previous studies have reported that various drug release mechanisms have been realized by incorporating a range of excipients into the outer shell of the dry-coated tablet (Lin et al., 2004). The dry-coated tablet is typically manufactured utilizing a two-step compaction process where the inner core precedes the outer coating compaction in a specialized tablet press. The resulting approach eliminates some unit operations, including granulation and/or coating, while also contributing to new manufacturing challenges due to added method complexity. In general, the optimal design of the outer layer is critically essential in reaching the predetermined delivery site via systemic circulation within tolerable drug concentrations. The geometric and mechanical properties of the tablet, including core eccentricity, could substantially affect the release profile of the drug. In realizing the designed drug-release action and dissolution profiles of a dry-coated tablet in a repeatable manner, it is widely accepted that the core tablet must be placed in the geometric center of the tablet with minimal eccentricity (Ozeki et al., 2003; Lin et al., 2004). Thus the quality of dry-coated tablets is required to be closely monitored especially when the control of dissolution rates of their active ingredients are critically important, such as for drugs with narcotic ingredients.

Despite many dry-coated tablet designs strictly utilizing cores to transport the active ingredients, the use of both core and thick coats for delivery of active ingredients has also been adopted in many applications. Demonstrating the accurate formation of the outer layer and thickness uniformity are paramount to the successful performance of the tablet in the drug release pattern and dissolution profile required for optimal therapeutic delivery. Also it has been previously reported that various lag-times (i.e., drug release initiating time) in the release pattern of dry-coated tablets can be achieved by simply altering the thickness of the outer coat later. Leading to the conclusion that if the core tablet can be placed precisely in the center of the whole dry-coated tablet with limited eccentricity, then the accuracy of the aforementioned drug release effects can be optimized only by precise manufactured thicknesses of the dry coat (Ozeki et al., 2003); emphasizing the importance of knowing the geometric position of the core tablet to the pharmaceutics manufacturing and quality control process.

* Corresponding author. Tel.: +1 315 268 6514; fax: +1 315 268 6695.
E-mail address: cetin@clarkson.edu (C. Cetinkaya).

0378-5173/$ – see front matter © 2011 Elsevier B.V. All rights reserved.
doi:10.1016/j.ijpharm.2011.05.029

It has been reported that, as with any other classes of tablet designs, physical properties, such as Young's modulus and mass density, of the outer layer of dry-coated tablets are the important factors playing roles in its controlled drug release pattern (Takeuchi et al., 2000). For dry-coated tablets with specific outer layer thicknesses, the lag-time is determined by the outer layer erosion rate; depending directly on the mechanical strength following compaction. Conclusively, identifying the mechanical properties of the outer layers is a quintessential asset in manufacturing, quality monitoring, and predictive therapeutic design of the tablet.

Mechanical and geometric property characterization of dry-coated tablets with air-coupled and direct contact ultrasonic techniques is investigated in Akseli and Cetinkaya (2008) and Liu and Cetinkaya (2010) respectively, and it is concluded that the mechanical properties and thickness of the outer layer of dry-coated tablets can be obtained with the utilization of a nondestructive acoustic pulse–echo method. Considering the millisecond (ms) time-scale dwell time of a typical commercial compaction press (from ~5 ms to 80+ ms) (Levin, 2002) and the micro-seconds of pulse duration and time-of-flight (TOF) of an acoustics pulse in typical tablets, the results reported in Akseli et al. (2008a) and later Leskinen et al. (2010) indicates that the ultrasonic approach has potential to be employed for real-time in-die online monitoring of the geometric and mechanical properties of drug tablets. It is widely known that dwell-time is a key parameter defining the end-mechanical properties of the compacted tablet, such as hardness and porosity. For pharmaceutical applications, uses of a wide-spectrum of acoustic techniques for investigating the tablet hardness with ultrasonic methods (Lum and Duncan-Hewit, 1996), the effects of tablet porosity and particle size fraction of compacted on acoustic properties of tablets (Hakulinen et al., 2008), acoustic emission during compaction (Serris et al., 2002), their potential in identifying counterfeit tablets (Medendorp and Lodder, 2006), elasticity, integrity and defect states of tablets (Ketolainen et al., 1995; Varghese and Cetinkaya, 2007; Akseli et al., 2008b, 2009), and mechanical characterization of multi-layer tablets (Akseli et al., 2010) have been reported.

The objective of the current study is to demonstrate the feasibility and effectiveness of an in-die real-time online tablet quality monitoring system for dry-coated tablets by integrating the traditional die-punch set with an ultrasonic pulse–echo measurement system. The critical element of such a monitoring system is its ability to capture reflection waveforms from interfaces as pulses propagate from the embedded transducer into the die-punch materials and components of the tablet. In case of quality monitoring of dry-coated tablets, the key challenge is to detect the waves reflected from the coat–core interface and to extract the TOF data from this acquired waveform. The source of this difficulty is the fact that the amplitudes of the acquired waves are extremely low due to the high acoustic impedance mismatches between tablet and die/punch materials, and the transmission into the core is strong due to the slight acoustic impendence difference between the materials of the tablet coat and core. Thus, in addition to a sound experimental set-up, signal processing techniques are required for accurately extracting wave arrival times. Depending upon the specific objectives of a measurement task and/or the nature and accuracy of the known material properties of involved materials, the measured TOFs can be utilized for determining the coat thickness, mechanical properties of the coat material, and eccentricity of the core with respect to the outer boundaries of the tablet. In quality assessment, the quality of coat and the integrity of core–coat bonds as well as other defects leading to delamination and capping can also be monitored from the temporal attributes of acquired waveforms. Additionally, using a monitoring system based on the described measurement approach with a set of embedded transducers in the die and punches: layer thicknesses, material properties, the mechanical integrity, and the geometrical consistency (e.g., core eccentricity) of dry-coated tablet components can be determined and monitored real-time during compaction.

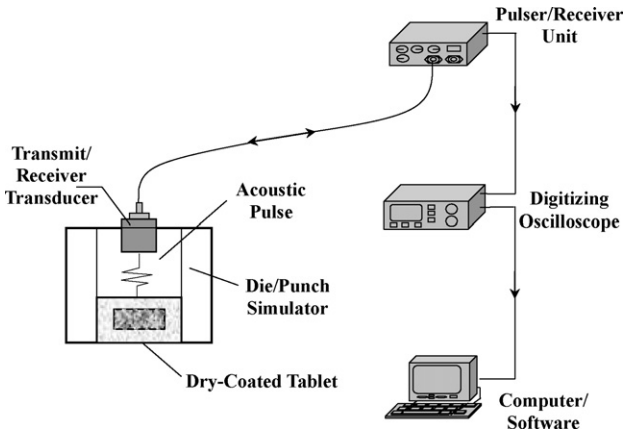

Fig. 1. Instrumentation diagram of the experimental pulse–echo measurement set-up (not to scale).

The characterization of geometric and mechanical properties of tablets as well as integrity in real-time is of interest to a wide spectrum of stakeholders, from the pharmaceutical manufacturing industry to regulatory agencies, as these parameters are directly related to tablet "hardness", porosity (solid fraction), and the overall quality of the end-product. In addition to the obvious impact in pharmaceutical manufacturing, the described real-time in-die approach supports the main objectives of the Quality by Design (QbD) and Process Analytical Technology (PAT) initiatives of the U.S. Food and Drug Administration (FDA), which is intended to analyze, and control manufacturing through timely measurements (i.e., during processing) of critical quality and performance attributes of raw and in-process materials and processes with the goal of ensuring final product quality (Hussain et al., 2004).

2. Experimental set-up and materials

The instrumentation diagram of the pulse–echo data acquisition experimental set-up used for acquiring reflection waveforms is included in Fig. 1. The experimental set-up consists of a pulser/receiver unit (Panametrics 5077PR), a digital oscilloscope (Tektronix TDS 3052), a commercial transducer (Panametrics V129) with the central frequency of 10 MHz, a set of acoustically characterized model medium materials used as delay lines and a personal computer with data analysis and processing software. The pulser/receiver unit generates a series of electrical square pulses with the prescribed values for pulse duration, voltage amplitude and pulse repetition frequency (PRF). As a result, the ultrasonic transducer generates acoustic pulses in a bandwidth around its resonance frequency as it is excited by the electrical pulses. The reflections and/or transmissions of the acoustic waves from a test piece interface is detected by the same transducer (pulse–echo mode) or another transducer (pitch–catch mode), and the resulting strain field is converted into electrical pulses (generated due to electric field–strain field coupling) that are received by the pulser/receiver unit and are transmitted to the digitizing oscilloscope to be saved as digitized waveforms for further analysis and signal processing. In the reported experiments, the data sampling frequency of the oscilloscope was set to 100 MHz at the averaging rate of 256 and the pulse repetition frequency of 5 kHz. The experimental set-up for pulse–echo measurements developed to obtain the TOF of the longitudinal (pressure) pulse transmitted into a dry-coated tablet and reflected from the interfaces of the sample tablet back to the originating transducer is depicted in Fig. 1.

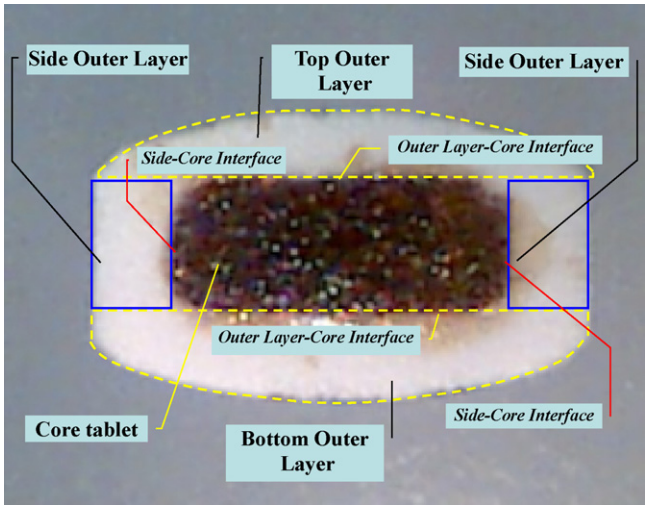

Fig. 2. The vertical cross-section view of a sample dry-coated tablet with its structural components (core and coat layers) and interfaces. The core is colored for visualization purposes. (For interpretation of the references to colour in this figure legend, the reader is referred to the web version of this article.)

Using signal processing techniques, the acquired waveforms by the pulser/receiver unit are analyzed to extract various types of temporal and amplitude information and eventually to determine the TOF in a specific layer of the tablet. In the current study, the TOF refers to the round trip TOF in a layer.

Since the acoustic impedance (Z) between a typical tooling material and tablet is markedly large, in current study, three types of medium materials with varying acoustic impedances, such as Lucite (Poly(methyl methacrylate) (PMMA)), aluminum, and stainless steel are utilized in the experimental set-up; simulating the materials and structure of a die-punch set. Lucite is employed due to its inherently low acoustic impedance, thorough acoustic properties characterizations, and the utilization by previous experiments in X-ray compaction monitoring. Despite the low correlation to real in-die compaction, which utilizes metallic and/or ceramic fixtures, the use of Lucite remains a legitimate choice for baseline comparisons.

A vertical cross-sectional image of a sample dry-coated tablet used in the reported experiments consisting of a core tablet and an outer (coat) tablet is depicted in Fig. 2. The core tablet is chemically darkened to identify its boundaries. In the current study, the outer tablet (coat) is composed of three structural components, namely the top outer layer, the bottom outer layer and the side outer layer. As reported in Liu and Cetinkaya (2010), the mechanical properties of the top and side layers could be substantially different even though they are made of the same powder. As indicated in Fig. 2, the three structural parts of the outer tablet coupled with the core form three interfaces (the top outer layer–core interface, the bottom outer layer–core interface and the side outer layer–core interface). In dry-coated tablet manufacturing, due to substantial centrifugal and vibrational forces generated in the rotary compaction presses, monitoring the position of the core tablet is critically important for ensuring the required symmetry of the tablet geometry. The mechanical properties are also as relevant as the geometrical properties; where the dissolution rates dependency on mechanical properties has been a well known phenomenon for a long time (e.g., see Higuchi et al., 1953a,b).

In the reported experiments, a set of 25 experimental dry-coated tablets each with the total nominal mass of 360 mg is utilized. The core and coat of the experimental tablets were compacted specifically for current study in a Manesty DryCota press (OYSTAR USA, Fairfield, NJ) from two undisclosed proprietary powder materials. The structural components (core and coat) and the interfaces of the sample tablets are shown in Fig. 2. Typical geometric and mechanical properties of the sample tablets are given as follows (Liu and Cetinkaya, 2010: the tablet mass density range is 1100–1150 kg/m^3, the thicknesses of the top and bottom coat layers are 1.2 mm and 1.6 mm, respectively, due to the known core eccentricity in the tablet, the average mass density of the top layer is 1144.9 kg/m^3, the travel times of pressure waves in the top and bottom layers are 1.05 μs and 1.40 μs respectively, the tablet diameter is 9.6 mm, the tablet thickness is 5.2 mm, the core diameter is 6.7 mm, and the core thickness is 2.4 mm. In each experiment, a fresh sample tablet is used to eliminate the effect of tablet material degradation due to the penetration of the acoustic couplant gel into coat and/or core materials and the associated effect on TOF measurements. The top layers of the tablets are filed flat to various levels to enhance the medium material to tablet contact area. The tablets in the sample set are divided into three groups. The first group, Group 1, consists of 5 tablets to be used with the Lucite medium. The second group, Group 2, consists of 10 tablets to be used with the aluminum medium, and finally the last group, Group 3, consists of 10 tablets to be used with the steel medium. The acoustic couplant (Ultragel II) acts as an interfacial medium that conforms to the surface roughness features of the tablet; allowing acoustic energy transmission across the boundary. The waveforms and measurement results of the first sample tablet in each group is included and discussed, followed by Table 2 which depicts the entire data range of each group.

3. Experimental procedures

In demonstrating the ability to acquire and differentiate between weak reflection waves from the outer layer–core interface of a dry-coated tablet in the die, the noise floor, and other mixed reflected/scattered waves, the following three types of waveforms are acquired and processed for each tablet: (i) a Type I waveform contains the reflection pulses directly from the outer layer–core interface of the dry-coated tablets excluding a medium material (see Fig. 3a for the experimental schematics, and Figs. 4a, 5a, and 6a for sample Type I waveforms) for the purpose of obtaining the TOF in the outer layer of the tablet for verification purposes only, (ii) Type II is a waveform containing reflection pulses from only the medium material–air interface, excluding the tablet, to obtain the round-trip TOF in the medium material (Figs. 4c, 5b and 6b show sample Type II waveforms), and (iii) Type III is a waveform containing reflection pulses from the outer layer–core interface, and the medium–outer layer interface (see Fig. 3b for the experimental schematics and Figs. 4c, 5c, and 6c for sample Type III waveforms). The Type II and Type III waveforms are utilized to determine TOF in the outer layer, while the Type I waveform is used only to verify this TOF result. The purpose of using Type II and Type III instead of only Type I is obviously due to the physical configuration of the tablet in die requiring a pressure applying medium (i.e., punch tip) between transducer face and tablet. Understanding the physical configuration also brings into perspective the difficulty in acquiring signals from reflected boundaries in the outer layer–core interface due to acoustic impedance mismatch between tablet and medium material; resulting in low transmission coefficients, and thus low signal-to-noise ratios in the Type III waveform.

The TOF in the outer layer (T_{tof}) and medium material (D_{tof}) are obtained directly from the Type I and Type II waveforms, respectively. Using the acquired T_{tof} and D_{tof} the expected TOF in the combination medium material and tablet (Type III) can be calculated ($T_{tof} + D_{tof}$). The purpose for approximating the Type III arrival time is twofold: (i) the amplitude of the signal acquired by Type III is typically comparable to the noise floor amplitude and requires sep-

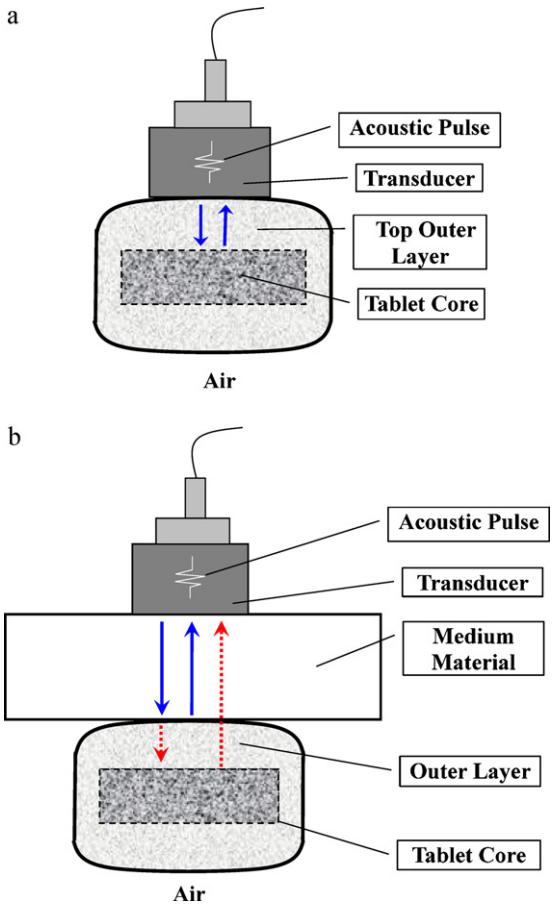

Fig. 3. Schematics of experimental configurations employed for acquiring: (a) a Type I waveform and (b) a Type III waveform for extracting the TOF in the outer layer of the dry-coated tablet. The Type II waveform (not shown here) is for the response of the medium material only.

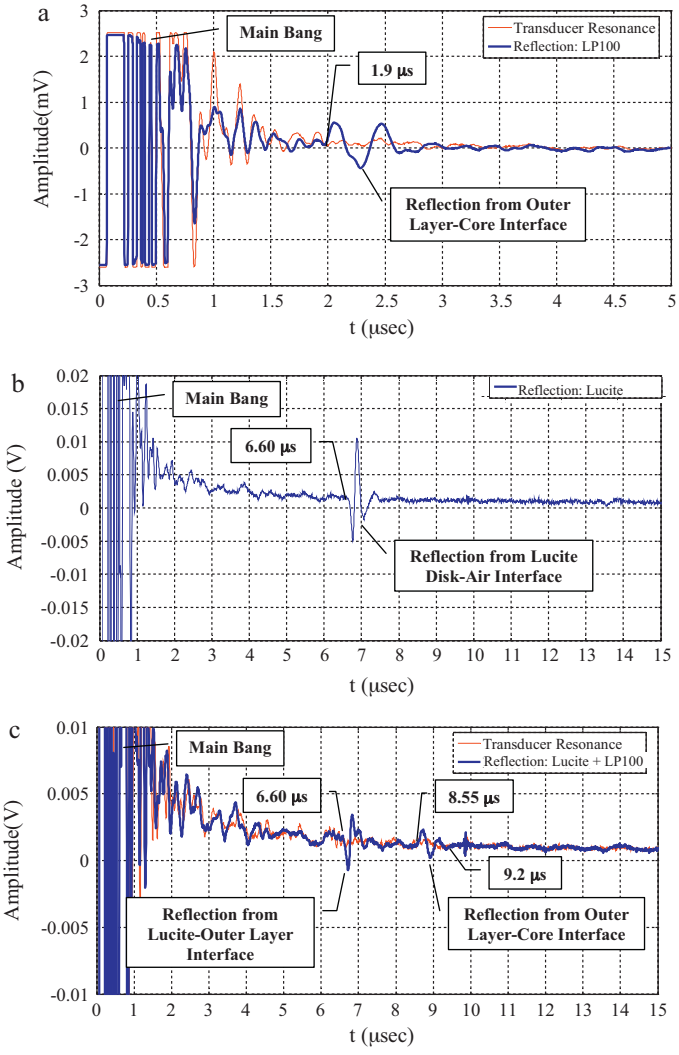

Fig. 4. Acquired Type I (a), Type II (b), and Type III (c) waveforms with the Lucite tooling medium material with labels indicating the arrival times of pulses corresponding to various interfaces.

arate signal processing effort to isolate. Coupled with the expected arrival time, the visual inspection assures the ability to utilize signal processing techniques to precisely determine the TOF in the outer layer. (ii) The second reason for approximating the time of arrival relates to confirming the actual method of determination during in-die monitoring: T_{tof} can be calculated by the difference of Type III waveform results ($T_{tof} + D_{tof}$), and Type II waveform results (D_{tof}). The difference method for calculation of T_{tof} is utilized in this study, and the results for T_{tof} from Type I waveforms are only for verification of the aforementioned difference method. If the difference of the expected value from the waveform Type I and the experimental value obtained in the waveform Type III are within a reasonable range, it can be concluded that (i) it is possible to obtain the reflection pulse from the outer layer–core interface of the dry-coated tablet in the transducer medium material-dry-coated tablet configuration, and (ii) it is possible to extract the relatively accurate TOF of longitudinal waves in the medium material and the outer layer of the tablet. Comparing the phases and amplitudes of the waveforms corresponding to the two configurations with and without the tablet, Type III and Type II respectively, could potentially reveal the TOF data if the reflection from the coat–core interface can be distinguished in the waveform for the configuration with a dry-coated tablet.

4. Experimental results and analysis

The medium materials made of Lucite, aluminum, and stainless steel, with experimentally determined characteristic acoustic impedances (Z) of 3.2MRayl (Z_L), 18MRayl (Z_A), and 66MRayl (Z_S) respectively, are used in the reported experiments. The acoustic impedance (Z) is defined as $Z = \rho c_L$, where ρ is the material mass density, and c_L is the phase velocity of pressure waves in the medium. The reflection coefficient, $c_R^{1\to2}$, and transmission coefficient, $c_T^{1\to2}$, of pressure waves at the boundary between Medium 1 and Medium 2 due to an incident pressure wave are as follows:

$$c_R^{1\to2} = \frac{Z_1 - Z_2}{Z_1 + Z_2} \qquad c_T^{1\to2} = \frac{2Z_2}{Z_1 + Z_2} \tag{1}$$

where Z_1 and Z_2 is the acoustic impedances of Medium 1 and Medium 2, respectively. To demonstrate the necessity of comparing different medium materials, and the inherent difficulty associated with metallic media that are typically utilized for die/punch materials, a representative value for the acoustic impedance of the outer tablet coat (Z_T) is assumed to be 1.8MRayl. Resulting in the following transmission (c_T) and reflection coefficients (c_R) between the medium material and the outer coat, as calculated using Eq. (1): $c_T^{L\to T} = 0.72$ and $c_R^{L\to T} = 0.28$, $c_T^{A\to T} = 0.17$ and $c_R^{A\to T} = 0.83$, $c_T^{S\to T} = 0.05$, and $c_R^{S\to T} = 0.95$, for Lucite (L), aluminum (A), and steel (S) respectively. Clearly, steel (and to a lesser extent aluminum) exhibit a relatively high reflection coefficient and a small transmission into the outer coat. The problem is realized, herein, due to the

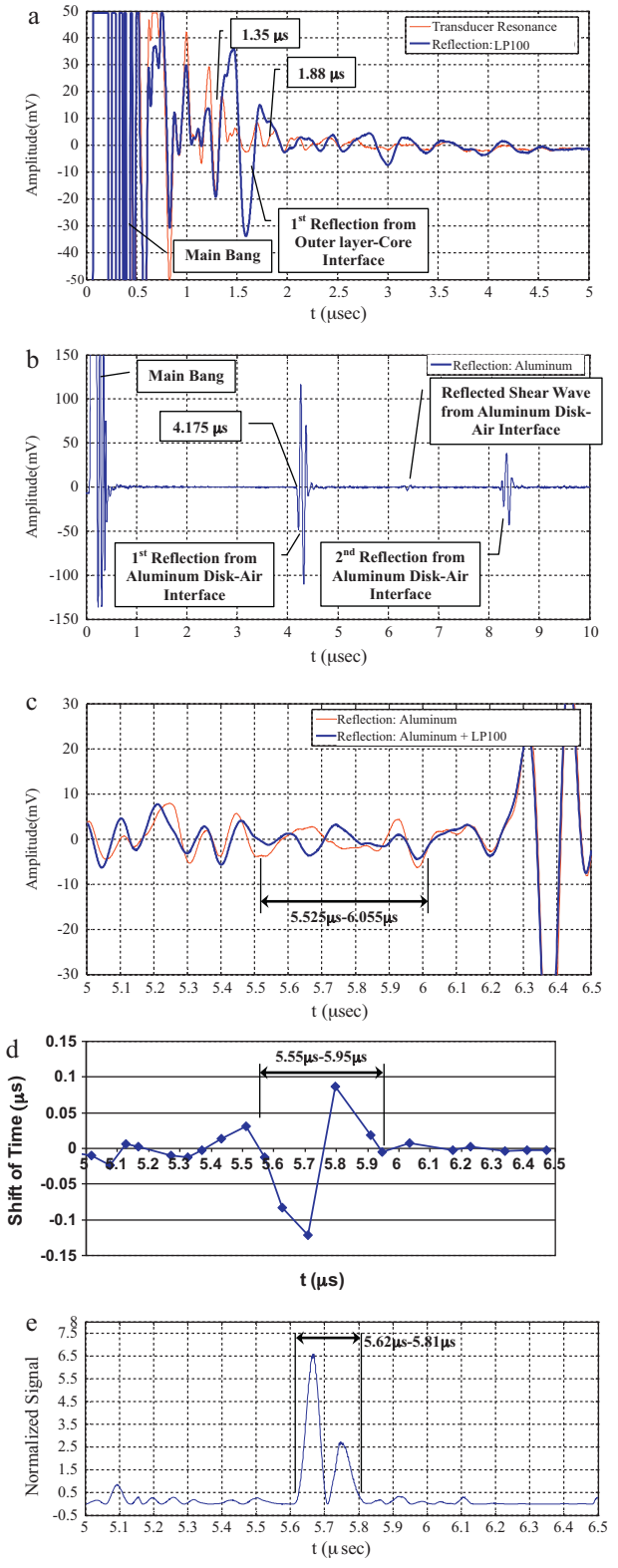

Fig. 5. Acquired Type I (a), Type II (b), and Type III (c) waveforms with the aluminum tooling medium material. The zero-crossing time-shift (d) and the normalized relative amplitude (e) plots corresponding to the phase and amplitude changes between the Type II and Type III waveforms.

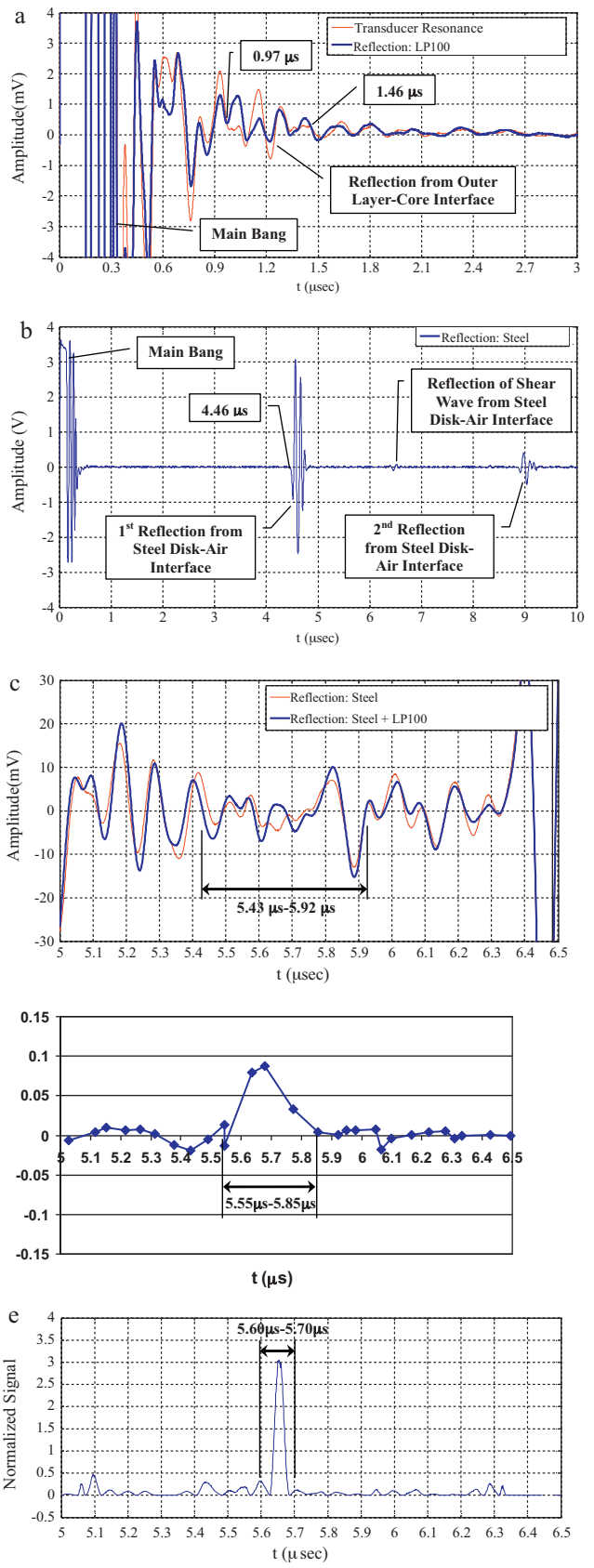

Fig. 6. Acquired Type I (a), Type II (b), and Type III (c) waveforms with the steel tooling medium material. The zero-crossing time-shift (d) and the normalized relative amplitude (e) plots corresponding to the phase and amplitude changes between the Type II and Type III waveforms.

low signal to noise ratio resulting from low amplitudes of reflected waves returning from the outer coat and inner core boundary.

To develop baseline comparison, wave propagation in a Lucite medium material was tested for characterizing the strength of the transmission and reflection pulses. In this medium, based on the similarity between acoustic impedances of the Lucite and tablet material, it is expected that the arrival time of the reflected pulse from the outer coat–inner core interface is sufficiently adequate to be observed in the Type III waveform. In the case of both aluminum and steel medium materials, a significant difficultly arises when attempting to distinguish and accurately identify the reflected pulse from the outer coat–inner core interface from the raw waveform (Type III), due to higher acoustic impendence mismatch, resulting in low amplitude reflected and transmitted pulses received at the transducer. In the current study it was ascertained that resulting amplitudes observed in the metal–air interface (approximately 230 mV for aluminum and 5.5 V for steel) are two to three orders of magnitude higher than the amplitudes observed in the metal–tablet interface (approximately 4 mV). The Lucite–tablet interface, comparatively, results in superior reflection amplitudes (Fig. 4c) than that of metals; further demonstrating the difficulty in resolving the reflection components by visual inspection in the metal–tablet interface (Figs. 5c and 6c). Additionally, the resulting reflection components of the waveforms from medium–air and medium–tablet interfaces (Type II and Type III) result in phase and amplitude changes due to mixing waveforms (i.e., signal degradation due to constructive and deconstructive interference), and a filtering effect caused by the frequency dependent attenuation; both of which prove useful for signal processing.

As previously established, realization of reflected wave arrival times is not a trivial problem due to the mixing of the medium–tablet interface and the outer coat–inner core interface reflections. Consequently, two basic signal processing methods are utilized to differentiate between coating and core arrival times. The first method, designated zero-crossing time shift technique, employs the phase shift observed in the waveforms to calculate arrival time. The second method, designated normalized relative amplitude difference technique, capitalizes on the amplitude differences associated with the mixing of reflected waves (Moon and Stirling, 2000). These techniques and associated algorithms are required for a computer controlled autonomous process monitoring and detection system to be developed for in-die monitoring. The zero-crossing time shift technique utilizes the phase difference (φ_s) between Type II and Type III waveforms by determining the discrete times the signals cross the time line at zero amplitude. The difference in zero crossing time between the Type II (Fig. 5b for aluminum and Fig. 6b for steel) and Type III (Fig. 5c for aluminum and Fig. 6c for steel) waveform is then plotted on a shift-of-time vs. time graph (Fig. 5d for aluminum and Fig. 6d for steel), and the TOF for the outer-layer can be realized by the difference in medium TOF (D_{tof}) and medium–outer coating TOF ($T_{tof} + D_{tof}$), as defined by:

$$T_{tof} = \Delta\varphi_s - D_{tof} \quad (2)$$

where T_{tof} is the TOF in the tablet, $\Delta\varphi_s$ the zero-crossing time shift technique determined TOF of the Type III waveform (equivalently $T_{tof} + D_{tof}$), and D_{tof} the TOF in the medium material as determined by the Type II waveform.

In the phase shift method (zero-crossing time shift technique), the phase difference (φ_s) between Type II and Type III waveforms is discreetly determined as a function of time as they are crossing the time line at zero amplitude. Waveforms in the Lucite medium have more obvious arrival features compared to the aluminum and steel mediums and require limited signal processing to visualize Types I–III depicted in Fig. 4a–c respectively. From Fig. 4c (Type III), by visual inspection, in the time range of 8.55–9.2 μs. The Type III reflection wave has the largest phase shift from the Type II reflection wave, indicating the location of mixing, and therefore the reflection from the outer layer–core interface. The results of the zero-crossing time shift technique for Lucite, aluminum, and steel are included in Tables 1 and 2.

As mixing of the waves occur in a particular portion of a Type III waveform, in addition to their phase, their amplitudes locally change and one approach to determine the temporal location of the coat–core reflected pulse in the waveform is to examine the changes in the amplitude. In this approach, here dubbed as the normalized relative amplitude difference technique, the normalized relative amplitude difference, not the absolute amplitude difference, is utilized. This is because the existence of the slight shift in the two waveforms makes the absolute amplitude difference less effective in distinguishing the two reflection waves. In this study, a simple amplitude norm is used, defined as:

$$A_n(t) = \left(\frac{f_3(t) - f_2(t)}{f_2(t)}\right)^2 \quad (3)$$

where $f_3(t)$ (Type III waveform) is the reflection wave from the coat–core interface using the setup of combined metal medium and dry-coated tablet, and $f_2(t)$ (Type II waveform) is the reflection wave of the metal medium only. This calculation is performed for the period of $f_2(t)$ and the resulting function $A_n(t)$ is plotted as a function of time $T_{tof} = A_n(t) - D_{tof}$, and a peak indicates in this plot the start time of the wave mixing, thus wave arrival.

The Lucite medium material utilized in the reported experiments is a cylindrical disk with a thickness of 8.82 mm and a diameter of 31.37 mm. From Fig. 4a, the TOF in the outer coat of the sample tablet (T_{tof}) from the Type I waveform is readily obtained: $T_{tof} = 1.9$ μs. The TOF in the Lucite disk (D_{tof}) is obtained from the waveform (Type II) in Fig. 4b: $D_{tof} = 6.60$ μs. Based on these two values, the expected TOF of pressure wave traveling through the Lucite medium and the outer coat of the sample tablet in the combination of transducer, medium material, and tablet (Type III) can be approximated as $T_{tof} + D_{tof} \cong 8.5$ μs. From Fig. 4c, the actual Type III TOF ($T_{tof} + D_{tof}$) of the pressure wave traveling in Lucite disk and the outer coat is determined to be $T_{tof} + D_{tof} = 8.55$ μs; deviating by only 0.6% from the expected value of ~8.5 μs. As also previously mentioned, the Lucite medium ideally reveals the reflected pressure pulses in the waveforms of the three types (I, II, and III) without necessitating the utilization of signal processing; proving advantageous for a visually ascertainable baseline comparison of the proceeding metallic medium setups.

The first metallic medium utilized to emulate the tooling materials (i.e., punch and die) is an aluminum disk with a thickness of 13.15 mm and a diameter of 50.83 mm. The purpose of utilizing a metallic medium is to determine the feasibility of obtaining and differentiating between reflection pulses in the waveforms, especially in the Type III waveform, when procuring reflections during in-die testing. The advantage of first testing an aluminum medium rather than a typical tooling material such as steel, is that the acoustic impedance of aluminum is roughly three times lower than steel (~18MRayl for aluminum and ~66MRayl for steel), which is closer to the approximated tablet acoustic impedance; thus allowing better transmission across the boundary between medium and tablet. To estimate the time of arrival in the Type III waveform, the process (as detailed in the experimental methods) utilizes the time of arrival in the Type I (T_{tof} between 1.35 μs and 1.88 μs as depicted in Fig. 5a) and Type II ($D_{tof} \cong 4.175$ μs as depicted in Fig. 5b) to estimate the arrival time in the Type III waveform ($T_{tof} + D_{tof}$) to occur between 5.525 μs and 6.055 μs, as depicted in Fig. 5c.

The waveforms utilizing a metallic medium require further signal processing due to a low signal to noise response of the reflected waves. The results of applying the zero-crossing time shift technique and the normalized relative amplitude technique are depicted in Fig. 5d and e respectively. The zero-crossing time

Table 1
TOF determination resulting in the medium only ($\boldsymbol{D}_{tof}$), medium–tablet ($\boldsymbol{T}_{tof}+\boldsymbol{D}_{tof}$), and effective coat layer ($\boldsymbol{T}_{tof}^{*}$) measurements for the three medium materials.

	Expected from combined Type II/III			Zero-crossing time shift technique			Normalized relative amplitude technique		
	$\boldsymbol{D}_{tof}$	$\boldsymbol{T}_{tof}+\boldsymbol{D}_{tof}$	$\boldsymbol{T}_{tof}^{*}$	$\boldsymbol{D}_{tof}$	$\boldsymbol{T}_{tof}+\boldsymbol{D}_{tof}$	$\boldsymbol{T}^{*}_{tof}$	$\boldsymbol{D}_{tof}$	$\boldsymbol{T}_{tof}+\boldsymbol{D}_{tof}$	$\boldsymbol{T}_{tof}^{*}$
Lucite	6.60	8.50	1.9	6.60	8.55	1.95	N/A	N/A	N/A
Aluminum	4.18	5.53	1.35	4.18	5.55	1.38	4.18	5.62	1.45
Steel	4.46	5.43	0.97	4.46	5.55	1.09	4.46	5.60	1.14

Table 2
The TOF data (top layer in bold font) for the tablet sample set using the zero crossing time shift and normalized relative amplitude techniques, including the mean and standard deviation of TOF (μ and σ) and direct-measured layer thickness (μ_d and σ_d).

Tablet no.	Group 1 TOF (μs) in lucite			Group 2 TOF (μs) in aluminum				Group 3 TOF (μs) in steel			
	Phase shift (±0.05)		Normalized amplitude (±0.01)	Phase shift (±0.05)		Normalized amplitude (±0.01)		Phase shift (±0.05)		Normalized amplitude (±0.01)	
1		1.95		**1.375**		**1.445**		**1.09**		**1.14**	
2		1.875			1.90		1.91	**1.15**		**1.17**	
3		1.91		**1.41**		**1.42**		**1.21**		**1.245**	
4	**1.415**			**1.395**		**1.41**			1.605		1.71
5	**1.44**				1.785		1.81	**1.085**		**1.295**	
6					1.80		1.86	**1.18**		**1.28**	
7					1.93		1.935		1.62		1.77
8				**1.44**		**1.45**			1.595		1.805
9				**1.425**		**1.435**			1.65		1.615
10				**1.36**		**1.42**		**1.205**		**1.29**	
μ (μs)	1.428	1.912		1.401	1.853	1.43	1.879	1.153	1.618	1.236	1.725
μ_d (mm)	1.21	1.62		1.18	1.56	1.21	1.59	0.97	1.36	1.04	1.46
σ (μs)	0.018	0.038		0.030	0.072	0.016	0.055	0.055	0.024	0.066	0.083
σ_d (μm)	14.4	31.3		25.3	60.8	11.8	46.5	46.5	20.3	55.8	70.1
σ/μ (%)	1.24	1.96		2.16	3.89	1.11	2.95	4.79	1.48	5.36	4.82

shift technique reveals a phase shifting event occurring between 5.55 μs and 5.95 μs, while the normalized relative amplitude technique reveals an amplitude differential occurring between 5.62 μs and 5.81 μs. The empirically determined (or calculably expected) arrival time from the combination of Type I and Type II results is again in the range of 5.525–6.055 μs. As a notable ranking, the zero-crossing time shift technique, Type I/Type II combination method, and normalized relative amplitude technique, in an ascending order of TOF range precision, accurately estimated the arrival times for every tablet utilized in the reported experiments; substantiating the legitimacy of the experimental setups and the integrity of the signal processing techniques developed for low signal to noise response detection presented in this report.

Finally, to confirm empirical and analytical experimental process robustness, a steel disk with a thickness of 12.58 mm and a diameter of 25.43 mm is utilized as a medium to simulate a typical punch and die tooling material. Briefly, the resulting time of arrival ranges from the Type I/Type II combination method (depicted in Fig. 6c), zero-crossing time shift technique (Fig. 6d), and normalized relative amplitude technique (Fig. 6e) are between 5.43 μs and 5.92 μs, 5.55 μs and 5.85 μs, and 5.60 μs and 5.70 μs, respectively. Notably, the Type III waveform for steel (Fig. 6c) lacks a distinguishable reflection pulse; relying entirely on the signal processing techniques to differentiate between the inherent noise of the system and the actual response from the reflection. Resulting in further legitimization of the experimental setup and signal processing techniques developed specifically for the purpose of time of arrival acquisition; especially when utilized for punch-die tooling material configurations.

The TOF measurement from the three sample tablets used for demonstration of waveforms and techniques are summarized in Table 1. In Table 1 the three columns of each determination method are: $\boldsymbol{D}_{tof}$ (Type II – the medium only), $\boldsymbol{T}_{tof}+\boldsymbol{D}_{tof}$ (Type III – the medium and tablet), and $\boldsymbol{T}_{tof}^{*}$ the effective TOF from the difference of Type III and Type II. The entire data set obtained using the 25 dry coated sample tablets is summarized in Table 2. Due to possible mechanical property alteration, as a result of couplant absorption, each sample tablet is utilized only once to minimize the effect. As a result, the data in Table 2 are differentiated between top layer TOF determination (bold font) and bottom layer TOF determination (regular font). The nominal thicknesses of the top and bottom layers are 1.2 mm and 1.6 mm respectively, and based on this manufactured core eccentricity, the orientation of the tablet samples are defined. The exact outer layer thicknesses of each sample tablet were determined by first splitting the tablets with a commercially available tablet splitter, and then measuring the top and bottom layer thicknesses with a 0.01 mm resolution micrometer (Mitutoyo CD-6″ CS). Also included in Table 2 are statistical figures indicating mean (μ) and standard deviations (σ) of both TOF and outer layer thicknesses.

5. Conclusions and remarks

A study for demonstrating the feasibility of characterizing the geometric/mechanical properties and integrity of dry-coated tablets (i.e., core eccentricity, compaction state of layers, and bonding state of interfaces) during compaction using an ultrasonic non-destructive approach was conducted. In the experiments, a set of 25 dry-coated tablets with known core eccentricity and compaction parameters were employed. The key problem in in-die compaction monitoring is the notable mismatch in acoustic impedance between the tooling materials (e.g., stainless steel) and the tablet material (pharmaceutical excipient); consequently limiting the signal to noise ratio experienced by the reflection pulses from the outer coat–inner core tablet layer. Two specially developed signal processing techniques and an experimental design utilizing various mock tooling materials (medium materials) enabled the isolation and capture of reflection waves from the interested tablet coat–core interface. Each method was developed and confirmed to facilitate the acquisition of reflection waves and the corresponding TOFs of the outer dry compaction coat layer during in-die compaction of dry coated tablets. Results of the current study indicate that employing an in-die system to actively monitor in-die tablet layer thicknesses, material properties, integrity of dry

coated tablet layer compaction state and bonding quality, and the core eccentricity is an achievable system. The characterization of tablet geometric and mechanical properties in a real time approach is of interest to the pharmaceutical manufacturing industry and to regulatory agencies; as these parameters are directly related to tablet hardness (affecting bonding and mechanical strength), porosity for its effect on dissolution profiles, and product quality (e.g., mechanical integrity). The preliminary substantiation of real-time in-die compaction monitoring supports the key objectives of quality monitoring and regulatory initiatives such as the Quality by Design (QbD) and Process Analytical Technology (PAT) of the U.S. Food and Drug Administration (FDA).

Uncitied reference

Akseli and Cetinkaya (2008).

Acknowledgements

Authors acknowledge Nicolas Michel and David Bohn of OYSTAR USA for providing sample tablets and funding for the initial phase of the presented experimental work. Thanks are also due to Dr. Ilgaz Akseli, a former graduate student (currently with Boehringer Ingelheim Corp.) and the undergraduate research student Carson J. Smith (Honors Program) at Clarkson University for their help with construction of experimental set-ups and data/signal processing.

References

Akseli, I., Cetinkaya, C., 2008. Drug tablet thickness estimations using air-coupled acoustics. Int. J. Pharm. 351, 165–173.
Akseli, I., Becker, D.C., Cetinkaya, C., 2009. Ultrasonic determination of Young's moduli of the coat and core materials of a drug tablet. Int. J. Pharm. 370, 17–25.
Akseli, I., Libordi, C., Cetinkaya, C., 2008a. Real-time acoustic elastic property monitoring of compacts during compaction. J. Pharm. Innovat. 3, 134–140.
Akseli, I., Mani, G.N., Cetinkaya, C., 2008b. Non-destructive acoustic defect detection in drug tablets. Int. J. Pharm. 360, 65–76.
Akseli, I., Dey, D., Cetinkaya, C., 2010. Mechanical property characterization of bilayered tablets using nondestructive air-coupled acoustics. AAPS PharmSciTech 11, 90–102.
Hakulinen, M.A., Pajander, J., Leskinen, J., Ketolainen, J., van Veen, B., Niinimaki, K., Pirskanen, K., Poso, A., Lappalainen, R., 2008. Ultrasound transmission technique as a potential tool for physical evaluation of monolithic matrix tablets. AAPS PharmSciTech 9, 267–273.
Higuchi, T., Narsimha Rao, A., Busse, L.W., Swintosky, J.V., 1953a. The physics of tablet compression. II. The influence of degree of compression on properties of tablet. J. Am. Pharm. Assoc. 42, 194–200.
Hussain, A.S., Watts, C., Afnan, A.M., Wu, H., 2004. Foreword. J. Process Anal. Technol. 1, 3–4.
Ketolainen, J., Oksanen, M., Rantala, J., Stor-Pellinen, J., Luukkala, M., Paronen, P., 1995. Photoacoustic evaluation of elasticity and integrity of pharmaceutical tablets. Int. J. Pharm. 125, 45–53.
Leskinen, J.T.T., Simonaho, S.P., Hakulinen, M., Ketolainen, J., 2010. In-line ultrasound measurement system for detecting tablet integrity. Int. J. Pharm. 400, 104–113.
Levin, M., 2002. Tablet Press Instrumentation, Encyclopedia of Pharmaceutical Technology. Marcel Dekker Inc.
Lin, S.Y., Lin, K.H., Li, M.J., 2004. Formulation design of double-layer in the outer shell of dry-coated tablet to modulate lag time and time-controlled dissolution function: studies on micronized ethylcellulose for dosage form design. AAPS J. 6, 1–6.
Liu, J., Cetinkaya, C., 2010. Geometric and mechanical properties of dry-coated tablets: contact ultrasonic techniques. Int. J. Pharm. 392, 148–155.
Higuchi, T., Narsimha Rao, A., Busse, L.W., Swintosky, J.V., 1953b. The physics of tablet compression. II. The influence of degree of compression on properties of table. J. Am. Pharm. Assoc.: Sci. Ed. 42, 194.
Lum, S.K., Duncan-Hewit, W.C., 1996. A comparison of elastic moduli derived from theory, microindentation, and ultrasonic testing. Pharm. Res. 13, 1739–1745.
Medendorp, J., Lodder, R.A., 2006. Acoustic-resonance spectrometry as a process analytical technology for rapid and accurate tablet identification. AAPS Pharm. 7, E1–E9.
Moon, T.K., Stirling, W.C., 2000. Mathematical Methods and Algorithms for Signal Processing, 1st ed. Prentice Hall, Upper Saddle River, NJ.
Takeuchi, H., Yasuji, T., Yamamoto, H., Kawashima, Y., 2000. Spray-dried lactose composite particles containing an ion complex of alginate-chitosan for designing a dry-coated tablet having a time-controlled releasing function. Pharm. Res. 17, 94–99.
Ozeki, Y., Watanabe, Y., Inoue, S., Danjo, K., 2003. Evaluation of the compression characteristics and physical properties of the newly invented one-step dry-coated tablets. Int. J. Pharm. 267, 69–78.
Serris, E., Perier-Camby, L., Thomas, G., Desfontaines, M., Fantozzi, G., 2002. Acoustic emission of pharmaceutical powders during compaction. Powder Technol. 128, 296–299.
Varghese, I., Cetinkaya, C., 2007. Non-contact photo-acoustic defect detection in drug tablets. J. Pharm. Sci. 96, 2125–2133.